 DOI: 10.1002/masy.200751309

Modeling Nd-Catalyzed Butadiene Rubber Production

Ursula Tracht,[*1] *Heike Kloppenburg*[2]

Summary: A simulation tool was developed for the industrial solution polymerization of 1,3-butadiene with a Nd-based homogeneous Ziegler-Natta catalyst system. Insight into underlying reaction mechanisms was gained from laboratory experiments. Besides the chain growth reaction, the following steps were identified: catalyst formation, deactivation reactions, and molecular weight control reactions. A kinetic model based on this reaction scheme was developed to quantitatively describe butadiene conversion and product molecular weight distribution. By including process characteristics, the laboratory (batch) model was transferred to the industrial production process. A correlation function relates product molecular weight to the relevant product property Mooney viscosity. This polymerization model was successfully applied, e.g. to optimize product grade transitions and to maintain high product quality by predicting the influence of process changes.

Keywords: kinetics; modelling; neodymium catalysis; polybutadiene; Ziegler-Natta polymerisation

Introduction

Nd-based homogeneous Ziegler-Natta catalyst systems are used in the industrial solution polymerization of 1,3-butadiene. A typical catalyst system comprises a Neodymium salt, a chlorinating and an alkylating co-catalyst. Lanxess is the major producer and supplier of butadiene rubber by Nd-catalysis (NdBR) for different applications like e.g. tire, golf ball and plastics industry. The quality and consistency of this NdBR and the corresponding end products are highly appreciated in the associated industries.

The objective of the work presented here is a simulation tool to be employed for even better product quality control, improved production process performance, operator training, and development of products with new property profiles. The concept of predicting product quality in industrial polymerization processes by means of mathematical models is applied to various polymerization types[1–3] however, to our knowledge no comprehensive model for Ziegler-Natta catalyzed butadiene polymerization can be found in the open literature. Development of a mathematical model that describes the dynamic evolution of monomer conversion, product molecular weight distribution and Mooney viscosity, as well as reactor temperatures (energy balance) for Nd-catalyzed butadiene polymerization is reported here. Thermodynamic data and reactor characteristics of the industrial solution polymerization process are available but reaction mechanism and kinetics for the butadiene polymerization with ternary Nd-based catalyst systems have not been fully elucidated so far. Two recent publications review the Nd catalyzed polymerization of 1,3-butadiene.[4,5] Parameters influencing the polymerization reaction are discussed, however, the information on reaction kinetics is limited. Available kinetic data cannot be directly transferred to the catalyst system and reaction conditions used here. Many kinetic studies, e.g.,[6,7] describe butadiene con-

[1] Bayer Technology Services GmbH, 51368 Leverkusen, Germany
E-mail: ursula.tracht@bayertechnology.com
[2] Lanxess Deutschland GmbH, 41538 Dormagen, Germany

sumption in terms of a pseudo first order rate law. This type of analysis yields effective rate coefficients for the overall reaction that depend on reaction conditions and catalyst concentration. Neither kinetic parameters nor detailed reaction schemes for the underlying reaction steps like catalyst formation and deactivation are deduced. Alternative approaches describe the overall reaction by a polynomial as a function of the concentrations of butadiene and all catalyst components.[8,9] Again, kinetic parameters for the underlying reaction steps are not obtained from this analysis. More detailed kinetic studies[10] do not cover the parameter range of our industrial polymerization process.

In the study reported here, dedicated laboratory experiments were performed to identify individual reaction steps and determine the corresponding kinetic parameters. Based on the laboratory results, a batch model was developed, transferred to the specific industrial process, and validated with process data and additional laboratory experiments. The model is implemented in the simulation package PREDICI® (CiT GmbH, Rastede, Germany), a user interface is realized using the CiT-Observer.

Experimental Part

Isothermal batch experiments are carried out in a stirred stainless steel laboratory batch reactor. Reaction temperatures are kept constant to within ±1 K. The reactions are started by addition of the catalyst components, the active catalyst forms in situ. Samples are withdrawn to monitor butadiene conversion (gravimetric) and changes in molecular weight distribution. Molecular weights are measured by gel permeation chromatography (GPC) with 1,4-polybutadiene calibration or with coupled light scattering and refractive index detection. The exclusion limit of the column system used is about 10^7 g/mol. The mobile phase is THF. Butadiene concentration during the reaction is also followed by on-line NIR-measurements, which is crucial at higher reaction temperatures when the high butadiene vapor pressure impedes representative sampling from the reactor. Reference experiments with a standard recipe and reaction temperature are used to check reactor and reagent status. Parameter variations (reaction temperature, concentrations, order of addition) are performed only when these reference experiments show the same activity. Reproducibility of experiments with the standard conditions is illustrated in Figure 1.

Materials from the industrial production process are characterized in terms of Mooney viscosity, ML1 + 4(100).

Reaction Mechanism and Kinetics

Different reaction steps occur during the polymerization of butadiene catalyzed by the ternary Nd-system (Nd-salt, chlorinating agent, alkylating agent), i.e. formation of active catalyst centers, chain growth, chain transfer, and deactivation reactions. Depending on reaction conditions and concentrations, the individual reaction steps influence butadiene conversion and product properties in different ways. Since the aim is to use the kinetic model for quantitative prediction of conversion and product properties as a function of reaction conditions and concentrations, a quantitative description of the individual reactions steps in terms of rate laws is required for a wide range of temperatures and reagent concentrations.

First of all, the temperature dependence of the overall reaction rate was analyzed. At low reaction temperatures, the conversion curves show an induction phase, see bottom curves in Figure 2a and Figure 1. Under these reaction conditions at short reaction times, catalyst formation dominates the overall reaction rate. Catalyst formation is discussed in more detail below. At higher reaction temperatures, see Figure 2b, the conversion curves show different trends: the initial reaction rate is high but with increasing conversion, the rate of reaction decreases stronger than expected for a reaction first order in butadiene concentration. A propagation rate law with reaction order in butadiene

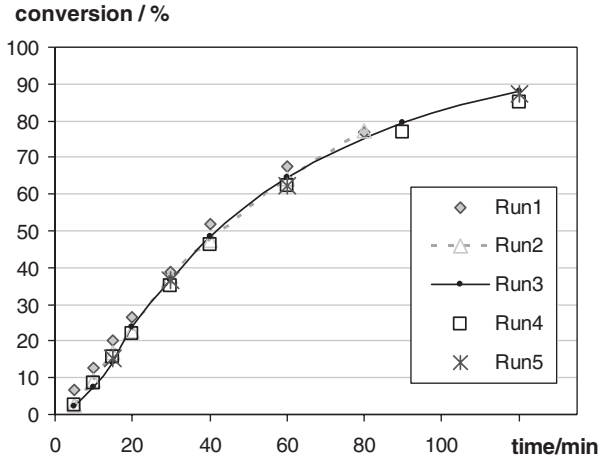

Figure 1.
Reproducibility of butadiene conversion from laboratory batch experiments at 60 °C and 10% butadiene in solution, standard catalyst concentration.

>1 can be excluded based on the lower temperature results. Experiments with different temperature profiles prove that the decrease in reaction rate with increasing temperature is due to thermal deactivation.

In order to gain insight into the mechanism of catalyst formation, the concentrations of the different catalyst components were varied. Figure 3 shows that the initial reaction rate increases with increasing concentration of chlorinating agent whereas the concentration of the second co-catalyst does not affect the overall reaction rate. The strong dependence of reaction rate on the concentration of chlorinating agent indicates that chlorination of the Nd compound is the rate determining step in catalyst formation. The reaction with the second co-catalyst (alkylation step) is much faster under all reaction conditions studied. Our results confirm a catalyst activation scheme like the one published in[11] consisting of alkylation and/or hydrogenation and chlorination steps. Figure 2 demonstrates that simulations with a kinetic model based on this catalyst formation scheme

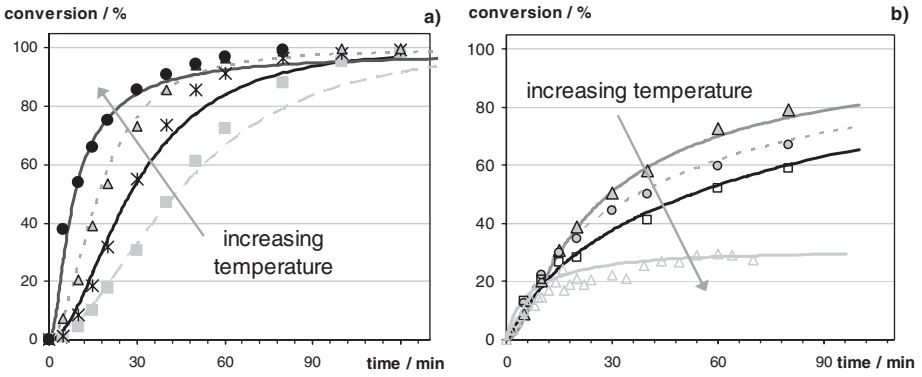

Figure 2.
Time dependence of butadiene conversion in isothermal laboratory batch experiments at different temperatures: a) low temperature range, b) high temperature range. Measured data (symbols) are compared to simulations (lines) with the kinetic model discussed in the text.

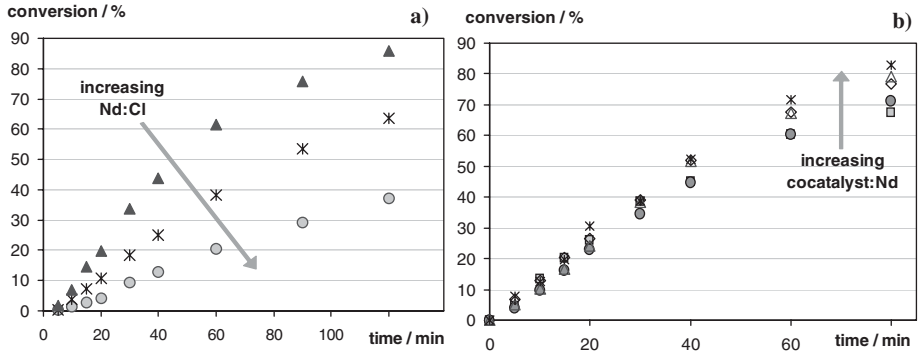

Figure 3.
Influence of the ratio of Nd precursor to a) chlorinating agent (varied by a factor of 2) and b) second cocatalyst (varied by a factor of 4) on overall reaction rate.

and including higher temperature deactivation reactions as well as different catalyst sites described below fit well to the experimental conversion data except for the lowest temperature analyzed. Kinetic equations and mechanistic schemes for the individual reactions of Nd based Ziegler-Natta polymerizations can be found in[11] and.[12] Simplified rate equations including the reaction steps that significantly influence butadiene conversion read

compositions and reaction temperatures. Butadiene conversion curves from low temperature experiments (ca. 40 experiments with variation of the concentrations of the three catalyst components and temperature, including replicates) are used for fitting $k_{\text{activation}}(T)$ and $k_{\text{propagation}}(T)$, validation of $k_{\text{propagation}}(T)$ and parameterization of all parameters related to deactivation processes are based on butadiene conversion from high temperature experi-

$$\frac{dc_{\text{active catalyst}}}{dt} = k_{\text{activation}}(T) \cdot c_{\text{Nd intermediate}} \cdot c_{\text{chlorinating agent}} - k_{\text{deactivation}}(T) \cdot c_{\text{active catalyst}}$$

$$\frac{dc_{\text{active catalyst 2}}}{dt} = f_2 \cdot k_{\text{activation}}(T) \cdot c_{\text{Nd intermediate}} \cdot c_{\text{chlorinating agent}} - k_{\text{deactivation}}(T) \cdot c_{\text{active catalyst 2}}$$

$$\frac{dc_{\text{butadiene}}}{dt} = -k_{\text{propagation}}(T) \cdot c_{\text{active catalyst}} \cdot c_{\text{butadiene}} - g_2 \cdot k_{\text{propagation}}(T) \cdot c_{\text{active catalyst 2}} \cdot c_{\text{butadiene}}$$

The equations are given for the model including two different active catalyst sites (see below). $c_{\text{active catalyst}}$ stands for the sum of free active catalyst concentration and active catalyst-polymer-complex concentration. For each of the reactions activation, propagation and deactivation, the same temperature dependence holds for both active sites. Only the pre-exponential factors of the rate coefficients $k_{\text{activation}}(T)$ and $k_{\text{propagation}}(T)$ are different as expressed by f_2 and g_2.

Figure 4 summarizes the temperature dependence of catalyst formation, chain growth, and thermal deactivation. The parameterization is based not only on butadiene conversion but also on product molecular weights for a wide range of ments (ca. 30 experiments). Fits to the corresponding molecular weight distributions (full temperature range) yield f_2 and g_2.

Product properties are primarily determined by molecular weight distribution. Figure 5 shows typical molecular weight distributions from isothermal batch experiments. All distributions are bimodal or even multimodal. For most experimental distributions satisfactory agreement of the measured distribution with a fit of two log-Gauss functions is achieved. In accordance with results published for various Nd-based catalyst systems,[4–7] the ratio of the two main fractions changes when the reaction conditions during catalyst formation are varied. This observation indicates

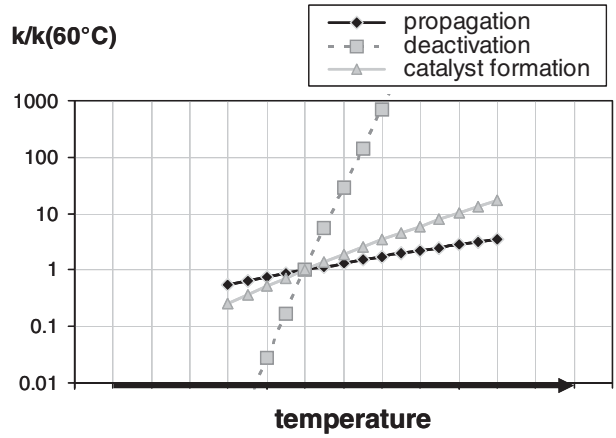

Figure 4.
Relative temperature dependence of the rate determining reaction steps, propagation, catalyst formation, and thermal deactivation.

that in our experiments (at least) two types of active centers are formed, as already anticipated in the rate equations given in the previous section. The two catalyst types not only differ in activity (propagation rate, model parameter g_2) but also in chain transfer properties. The molecular weight of the first fraction (at lower molecular weight) increases approximately linearly with butadiene conversion, see Figure 6. As Figure 6 also shows, the molecular weight of the lower molecular weight fraction can be controlled by the concentration of chain transfer agent. The linear dependence of M_n on conversion is sometimes classified as pseudo-living even though chain transfer and deactivation processes take place that are not consistent with true living behavior. Yet, the rather low polydispersity of this fraction of the molecular weight distribution and the linear growth with monomer conversion imply firstly that the chain transfer is reversible and fast on the time scale of the propagation reaction and secondly that deactivation is negligible at the temperature considered here. A mechanistic scheme for such a reversible chain transfer is proposed in.[11] The corresponding rate equation for a growing chain $P(s)$ of length s belonging to the lower molecular weight fraction (hence complexed to active catalyst of type 1) neglecting deactivation processes reads

$$\begin{aligned}\frac{dc_{P(s)}}{dt} = {} & k_{propagation}(T)\cdot c_{P(s-1)}\cdot c_{butadiene} \\ & - k_{propagation}(T)\cdot c_{P(s)}\cdot c_{butadiene} \\ & - k_{CT}(T)\cdot c_{P(s)}\cdot c_{CTA} \\ & + k_{CT\_back}(T)\cdot c_{P-CTA(s)}\cdot c_{P(r)}\end{aligned}$$

In contrast, the second fraction has a constant molecular weight regardless of butadiene conversion and chain transfer agent concentration. The constant molecular weight may be attributed to chain transfer processes to butadiene monomer or to a limited life-time and re-formation of the corresponding active sites. Simulations fit the experimental distributions best when the model assumes chain transfer to monomer. The amount of this second fraction relative to the lower molecular weight fraction remains approximately the same over the course of the reaction, thus both types of active sites must be active during the whole polymerization. Elucidation of the nature of the different active sites and their mechanism of formation were beyond the scope of this study. Quantitative modeling of experimental molecular weight distributions was achieved, see Figure 7, without a more detailed

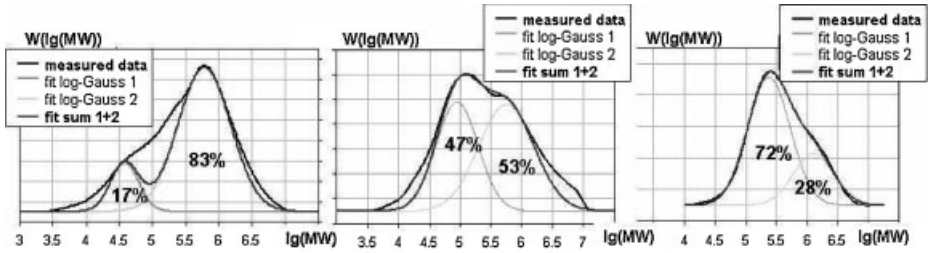

Figure 5.
Molecular weight (MW) distributions from three isothermal batch experiments at the same temperature and catalyst concentration but with different catalyst formation conditions. Experimental distributions in comparison to fits with two log-Gauss functions.

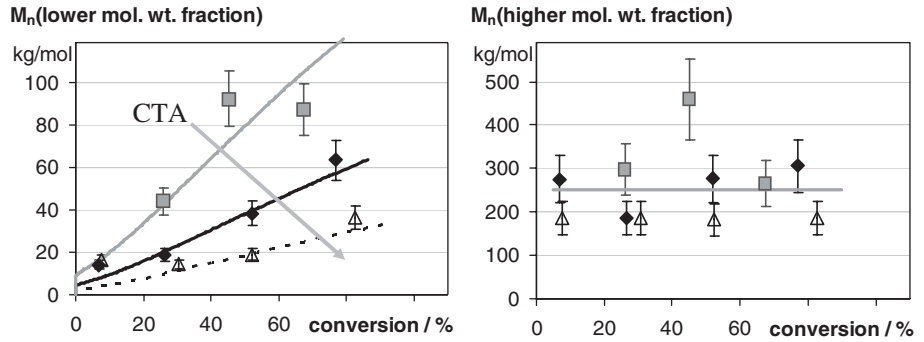

Figure 6.
Average molecular weights (M_n) for each of the two main fractions from fits to experimental molecular weight distributions. Experimental data (symbols) from three experiments with different chain transfer agent (CTA) concentrations are shown in comparison to simulations (lines).

description of the underlying mechanism of formation of the two catalyst sites included in the model. Formation of both sites at fixed relative rates, model parameter f_2, is assumed, and conversion of one type of active site into the other type cannot occur.

Results reported in the literature[5,13] and the observed dependence on reaction conditions in our experiments suggest that the active site that produces higher molecular weight polymer might be related to Nd agglomerates or heterogeneous catalyst fractions.

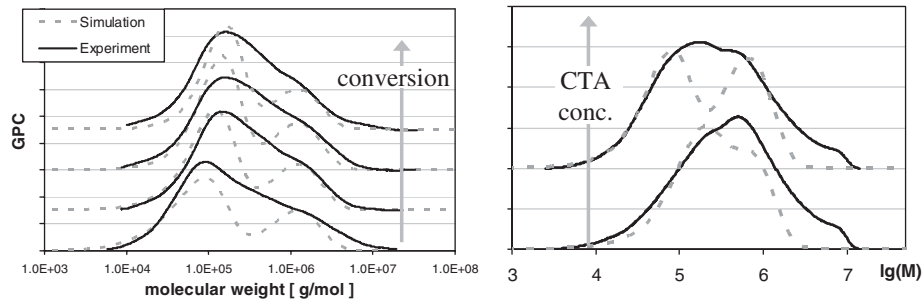

Figure 7.
Comparison of experimental GPC data to simulations for different butadiene conversions (left) and different concentrations of chain transfer agent (right).

The difference in molecular weight of the two main fractions indicates a difference in activity of the corresponding active site. Faster butadiene conversion in experiments that result in a distribution dominated by the higher molecular weight fraction supports this interpretation. However, neither catalyst activity nor chain transfer efficiency can be directly concluded from the molecular weights. Such analyses often used in kinetic model development are oversimplified in the case of the ternary Nd catalyst system studied here because the Nd precursor is not necessarily converted quantitatively into active sites, the ratio of the two active sites is not known, and molecular weights are influenced by chain transfer processes. The analysis of chain transfer processes is further complicated by the fact that one of the co-catalysts not only reacts with the catalyst but also acts as chain transfer agent and reacts with impurities so that the concentration of active chain transfer agent is not well defined. Because of these complex dependencies, reliable kinetic parameters cannot be inferred by only analyzing average molecular weights as a function of butadiene conversion and of catalyst component concentrations. Instead, our kinetic model is parameterized by simultaneously fitting simulated conversion curves and full molecular weight distributions to experimental data for a wide range of reaction conditions.

Figure 7 compares simulations for different butadiene conversions and for different concentrations of chain transfer agent to experimental GPC data. In all cases, the width of the experimental fractions is much larger than the simulated curves which indicates that in reality there is a distribution of catalytic activities rather than two types of active sites with well-defined activity. Neglecting these differences in distribution width, a satisfactory fit of experiment and simulation is obtained for the positions of the main fractions. The characteristics of experimental molecular weight distributions for a variety of reaction conditions are well described by two-site model.

Industrial Process Model

In order to apply the kinetic model to the industrial continuous polymerization, the reactor configuration, residence time distribution, and heat balance were accounted for. To illustrate the effect of residence time distribution and temperature profile, simulations for an ideal CSTR and a plug flow reactor are compared. For demonstration purpose, a hypothetic ratio of the two active sites corresponding to 60% lower molecular weight fraction was assumed. The same reaction volume and mass flow rate is used for both reactor types. In isothermal operation, higher conversion is reached in the plug flow reactor (98%) compared to the CSTR (93%), whereas for adiabatic operation similar conversions (90%) are reached in both reactor types because of the different temperature profiles. Figure 8 illustrates the simulated molecular weight distributions: as expected, the molecular weight distribution from a plug flow reactor is narrower due to the uniform residence time distribution. The actual residence time distribution in the industrial production plant is modeled by combinations of the ideal reactor types.

Product quality of NdBR is determined primarily by Mooney viscosity (a measure of molecular weight) and microstructure (content of 1,4-cis units). Extension of the kinetic model to include microstructure is in progress. Mooney viscosity prediction is

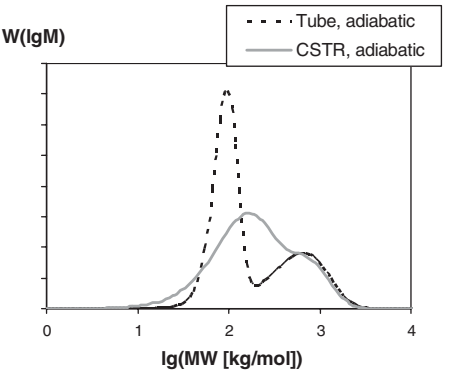

Figure 8.
Simulated molecular weight distributions for ideal reactor types.

achieved by correlating moments of the molecular weight distribution to Mooney viscosities. As discussed in,[14] a linear correlation between the logarithms of ML and of weight average molecular weight is expected but often other molecular weight averages give better correlations. We used well characterized laboratory samples spanning a large range of Mooney viscosities to establish the functional dependence, see Figure 9a–c. For the NdBR materials analyzed, the best correlation is obtained for a simple linear dependence of ML on M_n. With the same empirical functional dependence, good correlation between M_n from simulations with production data (feed streams) and experimental Mooney data for production samples is observed, Figure 9d. Perfect correlation is not expected for the production data covering about one year because unmeasured disturbances, e.g. impurities or uncertain measurements, always affect model predictions and cause varying offsets between simulation and measured Mooney viscosities. A single adjustable model parameter is introduced to account for the unmeasured disturbances by scaling chain transfer agent concentration and to a lesser extent also active catalyst concentration. Figure 10 illustrates that the dynamic mathematical model developed here reproduces well the observed industrial product characteristics.

Conclusions

A comprehensive kinetic model was developed for the polymerization of 1,3-butadiene

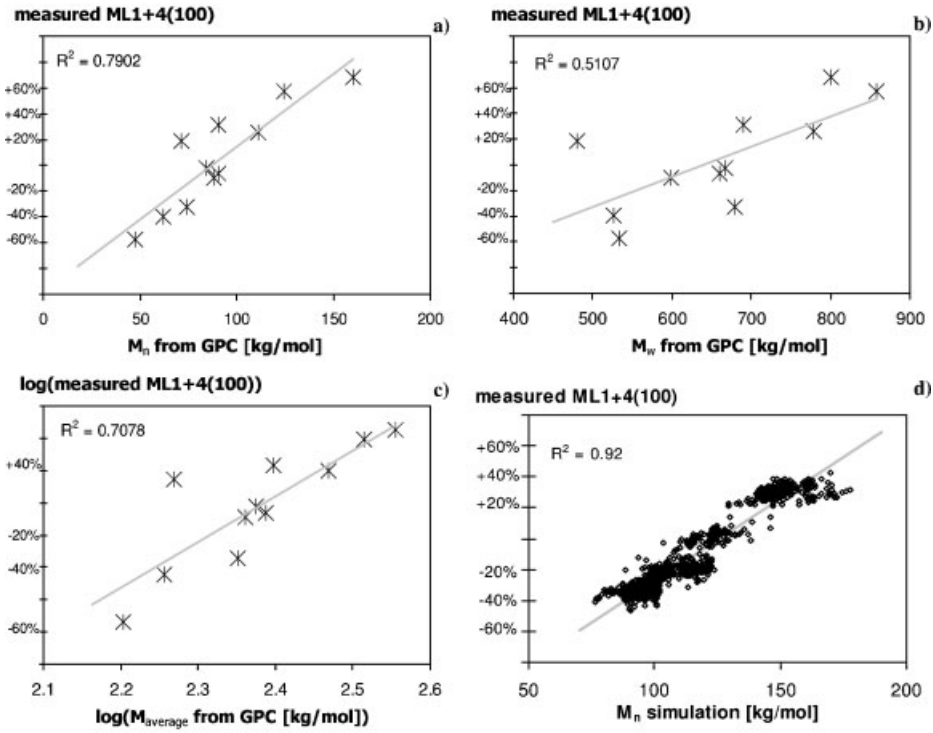

Figure 9.
Correlation between average molecular weights and measured Mooney viscosities: a) laboratory samples, number average molecular weight from GPC, b) weight average molecular weight from GPC, c) average molecular weight $(M_nM_w)^{0.5}$ from GPC data, d) M_n from simulations with production data (feed streams; constant adjustable model parameter in all simulations) for about 1 year of NdBR production.

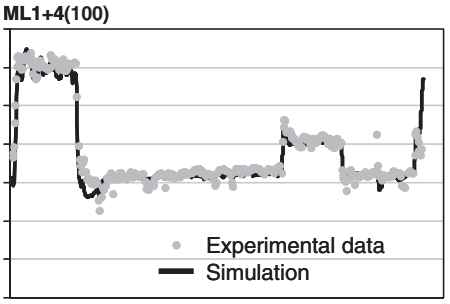

Figure 10.
Comparison of simulated to measured Mooney viscosities for production of different NdBR grades. Data cover a range of several weeks, all simulations with the same adjustable model parameter.

with a ternary Nd-based catalyst system. In contrast to previous models, not only the propagation reaction but also catalyst formation and deactivation reactions are included in the model and described quantitatively for a wide range of temperatures and concentrations. Butadiene conversion, full molecular weight distributions, Mooney viscosities, and reactor temperatures can be predicted with the polymerization model. Good agreement between measured Mooney viscosities for production samples and simulated data is achieved. The model is successfully applied to the industrial polymerization process for optimization of e.g. grade transitions or reactor configurations and for operator training.

Acknowledgements: Permission to publish this work from Lanxess, Business Unit BR, is gratefully acknowledged. The authors thank Dr. C. Mähner-Wolfarth for his support of the modeling project and experimental studies.

[1] C. Kiparissides, *Chem. Eng. Sci.* **1996**, *51*, 1637.
[2] M. Busch, *Macromol. Theory Simul.* **2001**, *10*, 408.
[3] C. Mähner, M. Hecker, DE10305579A1.
[4] I. L. Mello, M. B. Coutinho, B. G. Soares, D. S. S. Nunes, M. A. S. Costa, L. C. S. Maria, *Quim. Nova* **2004**, *27*, 277.
[5] L. Friebe, O. Nuyken, W. Obrecht, *Adv. Polym. Sci.* **2006**, *204*, 1.
[6] A. Oehme, U. Gebauer, K. Gehrke, M. D. Lechner, *Angew. Makromol. Chem.* **1996**, *235*, 121.
[7] A. Proß, P. Marquardt, K.-H. Reichert, W. Nentwig, T. Knauf, *Angew. Makromol. Chemie* **1993**, *211*, 89.
[8] R. P. Quirk, A. M. Kells, K. Yunlu, J.-P. Cuif, *Polymer* **2000**, *41*, 5903.
[9] A. Oehme, U. Gebauer, K. Gehrke, *Macromol Chem. Phys.* **1994**, *195*, 3773.
[10] G. A. Aminoa, G. V. Manuiko, V. V. Bronskaya, T. V. Ignashina, A. I. Ismagilova, G. S. D'yakonov, *Polym. Ser. A* **2006**, *48*, 881.
[11] L. Friebe, O. Nuyken, H. Windisch, W. Obrecht, *Macromol. Chem. Phys.* **2002**, *203*, 1055.
[12] P. Marquardt, "*Untersuchung und Modellierung der Polymerisation von Butadien mit Ziegler-Natta-Katalysatoren auf der Basis von Neodym*", Verlag Köster, Berlin **1994**.
[13] D. J. Wilson, D. K. Jenkins, *Polym. Bull.* **1995**, *34*, 257.
[14] O. Kramer, W. R. Good, *J. Appl. Polym. Sci.* **1972**, *16*, 2677.

